HALF INVERTED NESTED ARRAYS WITH LARGE HOLE-FREE FOURTH-ORDER DIFFERENCE CO-ARRAYS

Yuan-Pon Chen[1] *and Chun-Lin Liu*[2]

Dept. of Electrical Engineering[2], Graduate Institute of Communication Engineering[1,2]
National Taiwan University, Taipei, Taiwan 10617
r10942064@ntu.edu.tw[1] and chunlinliu@ntu.edu.tw[2]

ABSTRACT

Sparse arrays with fourth-order cumulant processing can identify up to $\mathcal{O}(N^4)$ source directions with only N physical sensors. To achieve this property, the fourth-order difference co-array is preferable to own a contiguous segment with no holes. However, existing sparse array designs either have holes in the co-array of size $\mathcal{O}(N^4)$ or own fewer than $\mathcal{O}(N^4)$ elements in the hole-free co-array. This paper proposes the half inverted nested array (HINA), which consists of a nested array and an inverted, scaled, and shifted nested array. By maximizing the size of the co-array, it can be shown that HINA with the optimal parameters possesses a hole-free fourth-order difference co-array of size $\mathcal{O}(N^4)$. Numerical examples demonstrate the improved DOA estimation performance of HINA.

***Index Terms*—** Sparse arrays, fourth-order difference co-arrays, nested array, direction of arrival estimation.

1. INTRODUCTION

In array processing, estimating the direction-of-arrivals (DOAs) of the incoming source signals is widely studied [1,2] and has been developed for decades. It is known that both the source statistics and the array configuration play a significant role in the estimation performance [3–5]. In particular, fourth-order cumulant data processing on sparse arrays is capable of resolving $\mathcal{O}(N^4)$ source DOAs with N physical sensors and statistically independent non-Gaussian source signals [6]. In contrast, the uniform linear array (ULA) only finds $\mathcal{O}(N)$ DOAs with the same number of sensors [7, 8]. The reason is that the fourth-order difference co-array, denoted by $\mathbb{D}_4$, has size $\mathcal{O}(N^4)$ for sparse arrays, but $\mathbb{D}_4$ is only $\mathcal{O}(N)$ for the ULA.

The structure of $\mathbb{D}_4$ is also critical to the applicability of DOA estimators. It is ubiquitous to deploy the variants of the multiple signal classification (MUSIC) algorithm on the cumulant information defined on $\mathbb{D}_4$ [6,9–13]. This co-array-based MUSIC algorithm attains the resolvability of $\mathcal{O}(N^4)$ DOAs for sparse arrays if the fourth-order difference co-array $\mathbb{D}_4$ contains a large central ULA segment $\mathbb{U}_4$ of size $\mathcal{O}(N^4)$. However, the co-array-based MUSIC algorithm [6] only takes the cumulant information on $\mathbb{U}_4$ and discards the information beyond $\mathbb{U}_4$. As a result, it is desirable to have a *hole-free* fourth-order difference co-array (i.e. $\mathbb{D}_4 = \mathbb{U}_4$) to fully exploit the information on $\mathbb{D}_4$ [13]. Furthermore, hole-free $\mathbb{D}_4$ results in a smaller aperture in the physical array, making it useful in scenarios where the physical aperture is fixed [14].

From this viewpoint, array configurations satisfying both $|\mathbb{U}_4| = \mathcal{O}(N^4)$ and $\mathbb{D}_4 = \mathbb{U}_4$ have been of considerable interest. In the literature, these properties on $\mathbb{D}_4$ were addressed by two families of sparse arrays. The first family of sparse arrays owns *a central ULA segment* $\mathbb{U}_4$ *of size* $\mathcal{O}(N^4)$, but there are holes in their $\mathbb{D}_4$. These arrays include the fourth-level nested array (FL-NA) [6], the sparse array extension with the fourth-order difference co-array enhancement based on the two-level nested array (SAFOE-NA) [15], the expanding and shift scheme with two nested arrays (EAS-NA-NA) [16] and that with large spacing (EAS-NA-NA_{LS}) [9], and the enhanced four-level nested array (E-FL-NA) [10]. Among these arrays, the EAS-NA-NA_{LS} achieves the largest $\mathbb{U}_4$ for sufficiently large N, but its $\mathbb{D}_4$ contains holes.

The second family of array geometries aims for *large hole-free* $\mathbb{D}_4$. This family contains the compressed nested array (CNA) [11], the two-level nested array for fourth-order-cumulant-based DOA (2L-FO-NA) [12], and the extended Cantor array based on fourth-order difference co-arrays (E-FO-Cantor) [13]. However, for these arrays, the size of $\mathbb{U}_4$ is compromised for the hole-free property $\mathbb{D}_4 = \mathbb{U}_4$. More specifically, for sufficiently large N, the size of $\mathbb{U}_4$ is $\mathcal{O}(N^2)$ for the CNA [11], $\mathcal{O}(N^2)$ for the 2L-FO-NA [12], and $\mathcal{O}(N^{3.17})$ for the E-FO-Cantor [13]. None of them achieves $|\mathbb{U}_4| = \mathcal{O}(N^4)$. Presented with these two families of array designs, sparse arrays satisfying $|\mathbb{D}_4| = |\mathbb{U}_4| = \mathcal{O}(N^4)$ remain open.

In this paper, we propose the half inverted nested array (HINA) to meet the property that $|\mathbb{D}_4| = |\mathbb{U}_4| = \mathcal{O}(N^4)$. HINA is composed of two nested arrays. The first half of HINA is a nested array aligned to the origin, while the second half of HINA is an inverted, scaled, and shifted nested array. With closed-form expressions of the parameters, HINA achieves a hole-free $\mathbb{D}_4$ for $N \geq 4$ sensors. Based on this result, we maximize the size of $\mathbb{U}_4$ of HINA with N sensors. According to the explicit expressions of the optimal parameters, $|\mathbb{U}_4|$ of HINA has an asymptotic expression of $N^4/64 = \mathcal{O}(N^4)$ for sufficiently large N. Note that the $|\mathbb{U}_4|$ of HINA is larger than that of the existing arrays with hole-free $\mathbb{D}_4$ [11–13]. The $|\mathbb{U}_4|$ of HINA is also comparable to that of the E-FL-NA, whose $\mathbb{D}_4$ has holes.

Paper outline: Section 2 first reviews DOA estimation with the fourth-order difference co-array, and then reviews the two-level nested array [17]. Section 3 defines HINA, proves the hole-free property of its $\mathbb{D}_4$, and derives the parameters that maximize $|\mathbb{U}_4|$. Section 4 compares several arrays in terms of the size of $\mathbb{U}_4$ and the DOA estimation performance. Section 5 concludes this paper.

2. PRELIMINARIES

Consider a linear array of N sensors. The sensors are located at $\ell_0\lambda/2, \ell_1\lambda/2, \ldots, \ell_{N-1}\lambda/2$, where $\ell_0, \ell_1, \ldots, \ell_{N-1}$ are integers

This work was supported in part by the Ministry of Science and Technology, Taiwan, under grant MOST 110-2222-E-002-007- and in part by the Ministry of Education, Taiwan, under the Yushan Young Scholar Program NTU-110V0902.

and λ is the wavelength of the incoming sources. The sensor locations are characterized by an integer set $\mathbb{S} = \{\ell_0, \ell_1, \ldots, \ell_{N-1}\}$.

Assume that there are D narrow-band sources impinging on $\mathbb{S}$ from angles $\theta_1, \theta_2, ..., \theta_D$. The received signal on the sensor at the location $\ell_m \lambda/2$ can be expressed as

$$x_m(t) = \sum_{d=1}^{D} e^{-j2\pi\ell_m\bar{\theta}_d} s_d(t) + n_m(t), \tag{1}$$

where $s_d(t)$ is the dth source signal, $\bar{\theta}_d = \frac{1}{2}\sin(\theta_d)$ is the normalized DOA as defined in [18], $n_m(t)$ is a zero-mean stationary Gaussian noise, and $m \in [\![0, N-1]\!]$. Here the notation $[\![a, b]\!] := \{a, a+1, \ldots, b\}$ for $a, b \in \mathbb{Z}$ with $a \leq b$. The source signals are assumed to be zero-mean, stationary, non-Gaussian, and statistically independent. The noise term is statistically independent of the sources. Next, we analyze the fourth-order circular cumulant of the received signals associated with the indices $n_1, n_2, n_3, n_4 \in [\![0, N-1]\!]$. The fourth-order circular cumulant of $x_{n_1}(t), x_{n_2}(t), x_{n_3}(t)$, and $x_{n_4}(t)$ is defined as [8, 19]

$$\begin{aligned}
&\mathrm{Cum}(x_{n_1}(t), x_{n_2}(t), x_{n_3}^*(t), x_{n_4}^*(t)) \\
&:= \mathbb{E}[x_{n_1}(t)x_{n_2}(t)x_{n_3}^*(t)x_{n_4}^*(t)] \\
&- \mathbb{E}[x_{n_1}(t)x_{n_2}(t)]\mathbb{E}[x_{n_3}^*(t)x_{n_4}^*(t)] \\
&- \mathbb{E}[x_{n_1}(t)x_{n_3}^*(t)]\mathbb{E}[x_{n_2}(t)x_{n_4}^*(t)] \\
&- \mathbb{E}[x_{n_1}(t)x_{n_4}^*(t)]\mathbb{E}[x_{n_2}(t)x_{n_3}^*(t)].
\end{aligned} \tag{2}$$

By (1), [6, Theorem 1], and the independence of the source signals and the noise term, the fourth-order cumulant in (2) becomes

$$\begin{aligned}
&\mathrm{Cum}(x_{n_1}(t), x_{n_2}(t), x_{n_3}^*(t), x_{n_4}^*(t)) \\
&= \sum_{d=1}^{D} e^{-j2\pi(\ell_{n_1}+\ell_{n_2}-\ell_{n_3}-\ell_{n_4})\bar{\theta}_d} c_d,
\end{aligned} \tag{3}$$

where $c_d = \mathrm{Cum}\{s_d(t), s_d(t), s_d^*(t), s_d^*(t)\}$. Note that the relation in (3) resembles the array model in (1). The quantity $\ell_{n_1} + \ell_{n_2} - \ell_{n_3} - \ell_{n_4}$ in (3) can be viewed as the locations on the virtual co-array. For this reason, we define the fourth-order difference co-array as follows [6].

Definition 1. For a linear array $\mathbb{S} = \{\ell_0, \ell_1, \ldots, \ell_{N-1}\}$, its fourth-order difference co-array $\mathbb{D}_4$ is defined as

$$\mathbb{D}_4 := \{\ell_{n_1} + \ell_{n_2} - \ell_{n_3} - \ell_{n_4} \mid n_1, n_2, n_3, n_4 \in [\![0, N-1]\!]\}.$$

By defining the notations $\alpha\mathbb{A} \pm \beta\mathbb{B} := \{\alpha a \pm \beta b | a \in \mathbb{A}, b \in \mathbb{B}\}$ for $\mathbb{A}, \mathbb{B} \subseteq \mathbb{R}$ and $\alpha, \beta \in \mathbb{R}$, $\mathbb{D}_4$ can also be expressed as $\mathbb{D}_4 = \mathbb{S} + \mathbb{S} - \mathbb{S} - \mathbb{S}$. We write $\alpha \pm \beta\mathbb{B} := \{\alpha\} \pm \beta\mathbb{B}$ for later use.

Based on $\mathbb{D}_4$, the central ULA segment $\mathbb{U}_4$ is defined to be the longest unit-spacing ULA in $\mathbb{D}_4$ with the element 0 included. More specifically, $\mathbb{U}_4 := [\![-U_4, U_4]\!]$ where $U_4 := \max\{m \in \mathbb{Z} \mid [\![-m, m]\!] \subseteq \mathbb{D}_4\}$. For more insight into the structure of $\mathbb{D}_4$, two other kinds of co-arrays are also defined here: the second-order difference co-array of $\mathbb{S}$ is defined as $\mathbb{D}_2 := \mathbb{S} - \mathbb{S}$, and the sum co-array of $\mathbb{S}$ is defined as $\mathbb{S}_2 := \mathbb{S} + \mathbb{S}$. By Definition 1, we obtain the relations that $\mathbb{D}_4 = \mathbb{D}_2 + \mathbb{D}_2 = \mathbb{S}_2 - \mathbb{S}_2$.

Next, we review the (two-level) nested array [17], which is a fundamental building block of HINA. A nested array with two parameters N_1 and N_2 is composed of a dense ULA with N_1 sensors and a sparse ULA with N_2 sensors. The parameters N_1 and N_2 are positive integers. With the left-most sensor aligned to the origin, $\mathbb{S}_{\text{NA}}$ is defined as

$$\mathbb{S}_{\text{NA}} := [\![0, N_1 - 1]\!] \cup \{(N_1 + 1)n - 1 | n \in [\![1, N_2]\!]\}. \tag{4}$$

Furthermore, the nested array possesses a large ULA segment in both its difference co-array $\mathbb{D}_{2,\text{NA}}$ and sum co-array $\mathbb{S}_{2,\text{NA}}$. These segments satisfy [17, 20]

$$\mathbb{D}_{2,\text{NA}} = \mathbb{S}_{\text{NA}} - \mathbb{S}_{\text{NA}} = [\![-(N_1+1)N_2 + 1, (N_1+1)N_2 - 1]\!], \tag{5}$$

$$\mathbb{S}_{2,\text{NA}} = \mathbb{S}_{\text{NA}} + \mathbb{S}_{\text{NA}} \supseteq [\![0, (N_1+1)(N_2+1) - 2]\!]. \tag{6}$$

3. HALF INVERTED NESTED ARRAY

3.1. Half Inverted Nested Array

Definition 2. Let $\mathbb{S}_{\text{NA}}^{(1)}$ be a nested array with parameters N_1 and N_2 and let $\mathbb{S}_{\text{NA}}^{(2)}$ be a nested array with parameters N_3 and N_4. Define $\mathbb{S}_{\text{I}} := \sigma(L - \mathbb{S}_{\text{NA}}^{(2)})$ to be the inverted array derived from $\mathbb{S}_{\text{NA}}^{(2)}$, where $\sigma := (N_1+1)(N_2+1) - 1$ and $L := (N_3+1)(N_4+1)$. The *half inverted nested array* (HINA) $\mathbb{S}_{\text{HI}}$ is defined as

$$\mathbb{S}_{\text{HI}} := \mathbb{S}_{\text{NA}}^{(1)} \cup \mathbb{S}_{\text{I}}.$$

HINA consists of two nested arrays, and the second one is adjusted. This design rule can also be seen in the EAS-NA-NA [16] and the G-FODC$_{\text{NA}}$ [21]. The second nested array of all three designs is scaled up by a factor, and that of HINA and the EAS-NA-NA is shifted. However, the second nested array of HINA (which takes up about *half* of HINA's sensors) is first *inverted* in the sense of having a negative sign in front of it. Besides, both the scaling factor and the shift offset of HINA are different from those of the EAS-NA-NA and the G-FODC$_{\text{NA}}$.

HINA can also be seen as the union of four ULAs with different spacing. This structure is similar to that of the four-level *nested array* (FL-NA) [6] and the E-FL-NA [10]. The FL-NA and the E-FL-NA have increasing spacing from the leftmost ULA to the rightmost one, while HINA has its third ULA with the largest spacing.

HINA has a total number of sensors $N = N_1 + N_2 + N_3 + N_4$, where $N_1 + N_2$ sensors are from $\mathbb{S}_{\text{NA}}^{(1)}$ and $N_3 + N_4$ sensors are from $\mathbb{S}_{\text{I}}$. Since N_1, N_2, N_3, and N_4 are all positive integers, HINA is only defined for $N \geq 4$.

Theorem 1. *HINA has a hole-free fourth-order difference co-array* $\mathbb{D}_{4,\text{HI}} = [\![-2L\sigma, 2L\sigma]\!]$.

Proof sketch. We first show that $\mathbb{D}_{4,\text{HI}} \subseteq [\![-2L\sigma, 2L\sigma]\!]$. This can be seen by that $\max(\mathbb{S}_{\text{HI}}) - \min(\mathbb{S}_{\text{HI}}) = L\sigma$, and hence the largest element and the smallest element of $\mathbb{D}_{4,\text{HI}}$ are $2L\sigma$ and $-2L\sigma$, respectively.

Next, we show that $\mathbb{D}_{4,\text{HI}} \supseteq [\![-2L\sigma, 2L\sigma]\!]$. Since any $\mathbb{D}_4$ is symmetric about 0, it suffices to show that $\mathbb{D}_{4,\text{HI}} \supseteq [\![0, 2L\sigma]\!]$. The interval $[\![0, 2L\sigma]\!]$ is divided into six disjoint sub-intervals:

$$\mathbb{I}_1 := [\![0, (L - N_3 - 1)\sigma - N_1 - 1]\!], \tag{7}$$
$$\mathbb{I}_2 := [\![(L - N_3 - 1)\sigma - N_1, (L - N_3 - 1)\sigma]\!], \tag{8}$$
$$\mathbb{I}_3 := [\![(L - N_3 - 1)\sigma + 1, L\sigma]\!], \tag{9}$$
$$\mathbb{I}_4 := [\![L\sigma + 1, (L+1)\sigma - N_1 - 1]\!], \tag{10}$$
$$\mathbb{I}_5 := [\![(L+1)\sigma - N_1, (L+1)\sigma]\!], \tag{11}$$
$$\mathbb{I}_6 := [\![(L+1)\sigma + 1, 2L\sigma]\!]. \tag{12}$$

To analyze $\mathbb{D}_{4,\text{HI}}$, we first consider the following difference co-arrays

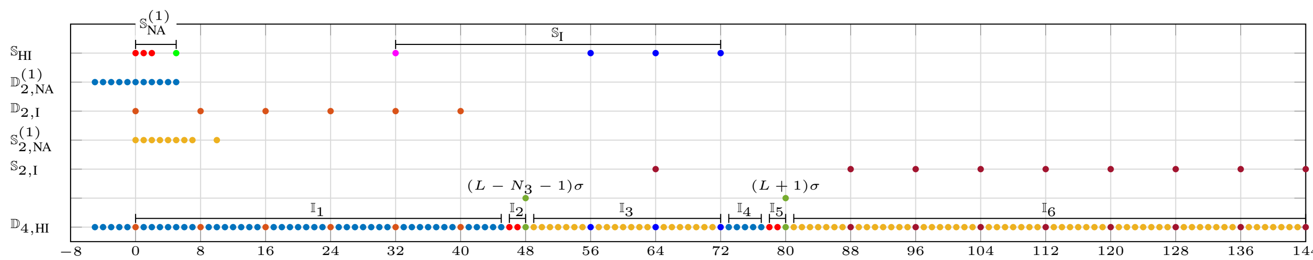

Fig. 1: An illustration of HINA $\mathbb{S}_{\mathrm{HI}}$ with $N_1 = N_2 = N_3 = N_4 = 2$ and the structure of the fourth-order difference co-array $\mathbb{D}_{\mathrm{HI}}$.

and sum co-arrays, according to (5), (6), and Definition 2,

$$\mathbb{D}_{2,\mathrm{NA}}^{(1)} := \mathbb{S}_{\mathrm{NA}}^{(1)} - \mathbb{S}_{\mathrm{NA}}^{(1)} = [\![-\sigma + N_1 + 1, \sigma - N_1 - 1]\!], \tag{13}$$

$$\mathbb{S}_{2,\mathrm{NA}}^{(1)} := \mathbb{S}_{\mathrm{NA}}^{(1)} + \mathbb{S}_{\mathrm{NA}}^{(1)} \supseteq [\![0, \sigma - 1]\!], \tag{14}$$

$$\mathbb{D}_{2,\mathrm{NA}}^{(2)} := \mathbb{S}_{\mathrm{NA}}^{(2)} - \mathbb{S}_{\mathrm{NA}}^{(2)} = [\![-L + N_3 + 2, L - N_3 - 2]\!], \tag{15}$$

$$\mathbb{S}_{2,\mathrm{NA}}^{(2)} := \mathbb{S}_{\mathrm{NA}}^{(2)} + \mathbb{S}_{\mathrm{NA}}^{(2)} \supseteq [\![0, L - 2]\!]. \tag{16}$$

By (15) and (16), the co-arrays of $\mathbb{S}_{\mathrm{I}}$ satisfy

$$\mathbb{D}_{2,\mathrm{I}} := \mathbb{S}_{\mathrm{I}} - \mathbb{S}_{\mathrm{I}} = \sigma[\![-L + N_3 + 2, L - N_3 - 2]\!], \tag{17}$$

$$\mathbb{S}_{2,\mathrm{I}} := \mathbb{S}_{\mathrm{I}} + \mathbb{S}_{\mathrm{I}} \supseteq 2L\sigma - \sigma[\![0, L - 2]\!]. \tag{18}$$

We also define the following sets

$$\mathbb{K}_1 := \mathbb{D}_{2,\mathrm{I}} + \mathbb{D}_{2,\mathrm{NA}}^{(1)}, \qquad \mathbb{K}_2 := (L - N_3 - 1)\sigma - \mathbb{S}_{\mathrm{NA,dense}}^{(1)},$$

$$\mathbb{K}_3 := \mathbb{S}_{\mathrm{I,dense}} - \mathbb{S}_{2,\mathrm{NA}}^{(1)}, \qquad \mathbb{K}_4 := L\sigma + \mathbb{D}_{2,\mathrm{NA}}^{(1)},$$

$$\mathbb{K}_5 := (L + 1)\sigma - \mathbb{S}_{\mathrm{NA,dense}}^{(1)}, \qquad \mathbb{K}_6 := \mathbb{S}_{2,\mathrm{I}} - \mathbb{S}_{2,\mathrm{NA}}^{(1)},$$

where $\mathbb{S}_{\mathrm{NA,dense}}^{(1)} := [\![0, N_1]\!]$ and $\mathbb{S}_{\mathrm{I,dense}} := \sigma(L - [\![0, N_3]\!])$ denote the dense ULA part of $\mathbb{S}_{\mathrm{NA}}^{(1)}$ and $\mathbb{S}_{\mathrm{I}}$, respectively.

With these notations, it can be shown that $\mathbb{K}_k \subseteq \mathbb{D}_{4,\mathrm{HI}}$ for $k \in [\![1, 6]\!]$, according to Definition 1 and the fact that $0, (L-N_3)\sigma, (L-1)\sigma, L\sigma \in \mathbb{S}_{\mathrm{HI}}$. Besides, by (13), (17) and the fact that $2(\sigma - N_1 - 1) + 1 \geq \sigma$, we obtain $\mathbb{K}_1 \supseteq \mathbb{I}_1$. By (13), (14), (18), it can be shown that $\mathbb{K}_k \supseteq \mathbb{I}_k$ for $k \in [\![2, 6]\!]$. Altogether, $\mathbb{D}_{4,\mathrm{HI}} \supseteq \cup_{k=1}^{6} \mathbb{K}_k \supseteq \cup_{k=1}^{6} \mathbb{I}_k = [\![0, 2L\sigma]\!]$. These arguments complete the proof. $\square$

Fig. 1 illustrates the proof of Theorem 1 with $N_1 = N_2 = N_3 = N_4 = 2$ and $\mathbb{S}_{\mathrm{HI}} = \{0, 1, 2, 5, 32, 56, 64, 72\}$. Each row in Fig. 1 illustrates the elements of the sets associated with the proof of Theorem 1. The four sub-arrays of $\mathbb{S}_{\mathrm{HI}}$ are colored differently in Fig. 1. According to the $\mathbb{S}_{2,\mathrm{NA}}^{(1)}$ and $\mathbb{S}_{2,\mathrm{I}}$ in Fig. 1, $\mathbb{K}_6 = \{54\} \cup [\![57, 64]\!] \cup \{78\} \cup [\![81, 144]\!]$, which is a superset of $\mathbb{I}_6 = [\![81, 144]\!]$.

The design of HINA utilizes the $\mathbb{D}_2$, the $\mathbb{S}_2$, and even the original structure of the two-level nested array. The coverage of $\mathbb{I}_1$ makes use of both $\mathbb{D}_{2,\mathrm{NA}}^{(1)}$ and $\mathbb{D}_{2,\mathrm{I}}$. This is based on the fact that $\mathbb{D}_4 = \mathbb{D}_2 + \mathbb{D}_2$, which is inspired by the G-FODC [21] and the EAS scheme [16]. On the other hand, covering $\mathbb{I}_6$ takes both $\mathbb{S}_{2,\mathrm{NA}}^{(1)}$ and $\mathbb{S}_{2,\mathrm{I}}$. This is based on the fact that $\mathbb{D}_4 = \mathbb{S}_2 - \mathbb{S}_2$, which only the EAS-NA-NA$_{\mathrm{LS}}$ takes into consideration [9]. Besides, the dense ULA parts of $\mathbb{S}_{\mathrm{I}}$ and $\mathbb{S}_{\mathrm{NA}}^{(1)}$ also play an important role in covering $\mathbb{I}_2$, $\mathbb{I}_3$, and $\mathbb{I}_5$.

3.2. Co-array Maximization of HINA

When the number of sensors N is fixed, it is preferable to maximize the central ULA segment of the co-array. Thus, we cast the following optimization problem for the parameters N_1, N_2, N_3, and N_4:

$$\max_{N_1, N_2, N_3, N_4 \in \mathbb{N}} \; U_{\mathrm{HI}}(N_1, N_2, N_3, N_4) \tag{19a}$$

$$\text{subject to} \quad N_1 + N_2 + N_3 + N_4 = N, \tag{19b}$$

where $U_{\mathrm{HI}}(N_1, N_2, N_3, N_4) := 2L\sigma$ denotes the U_4 of HINA.

Theorem 2. *One of the optimal solutions to* (19) *is*

$$(N_1^{\mathrm{opt}}, N_2^{\mathrm{opt}}, N_3^{\mathrm{opt}}, N_4^{\mathrm{opt}}) = \begin{cases} (k, k, k, k), & \text{if } N = 4k, \\ (k+1, k, k, k), & \text{if } N = 4k+1, \\ (k+1, k+1, k, k), & \text{if } N = 4k+2, \\ (k+1, k+1, k+1, k), & \text{if } N = 4k+3. \end{cases} \tag{20}$$

Proof sketch. This proof is inspired by the proof of [6, Theorem 3]. We first give the maximum difference between any two parameters, and then show that these parameters are roughly equally divided.

First, note that the parameters N_1 and N_2 in U_{HI} are interchangeable, and so are the parameters N_3 and N_4 in U_{HI}. More specifically,

$$U_{\mathrm{HI}}(N_1, N_2, N_3, N_4) = U_{\mathrm{HI}}(N_2, N_1, N_3, N_4) \tag{21}$$

$$= U_{\mathrm{HI}}(N_1, N_2, N_4, N_3). \tag{22}$$

Next, we claim that the optimal solutions to (19) cannot have any two N_i and N_j differing by more than 1. Due to the interchangeability between N_1 and N_2 in (21) and that between N_3 and N_4 in (22), it suffices to consider four cases only. We denote $\mathbb{S}_{\mathrm{HI}}(N_1, N_2, N_3, N_4)$ as HINA with the parameters N_1, N_2, N_3, and N_4 in what follows.

Case 1 is associated with the condition that $N_1 - N_3 \geq 2$. In Case 1, it can be shown that $\mathbb{S}_{\mathrm{HI}}(N_1 - 1, N_2, N_3 + 1, N_4)$ and $\mathbb{S}_{\mathrm{HI}}(N_1, N_2, N_3, N_4)$ share the same number of sensors. Furthermore, it can be shown that $U_{\mathrm{HI}}(N_1 - 1, N_2, N_3 + 1, N_4)$ is greater than $U_{\mathrm{HI}}(N_1, N_2, N_3, N_4)$. Namely, we can sequentially reduce $N_3 - N_1$ to increase the objective function in (19a) and to maintain the constraint in (19b) simultaneously. Therefore, the optimal solutions to (19) do not satisfy $N_1 - N_3 \geq 2$.

Case 2 considers the condition that $N_3 - N_1 \geq 2$. Similar to the argument in Case 1, it can be shown that $U_{\mathrm{HI}}(N_1 + 1, N_2, N_3 - 1, N_4)$ is greater than $U_{\mathrm{HI}}(N_1, N_2, N_3, N_4)$. Therefore, the optimal solutions to (19) do not meet the condition that $N_3 - N_1 \geq 2$. The same proof technique applies to *Case 3* ($N_1 - N_2 \geq 2$) and *Case 4* ($N_3 - N_4 \geq 2$).

In addition to Cases 1 to 4, the optimal solutions satisfy the condition that $N_2 \geq N_3$. This condition arises from the following argument. If $N_2 < N_3$, then it can be shown that $U_{\mathrm{HI}}(N_1, N_3, N_2, N_4)$ is greater than $U_{\mathrm{HI}}(N_1, N_2, N_3, N_4)$.

Next, with the constraints on the optimal solutions to (19), we let $(N_1^{\mathrm{opt}}, N_2^{\mathrm{opt}}, N_3^{\mathrm{opt}}, N_4^{\mathrm{opt}})$ be an optimal solution to (19). By (21)

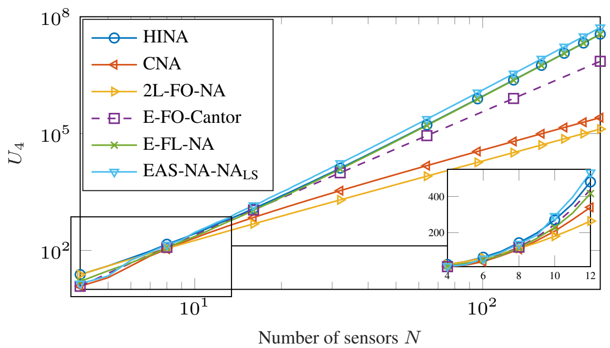

Fig. 2: The dependence of the parameter U_4 on the number of sensors for $N \in [\![4, 256]\!]$. For arrays other than the E-FO-Cantor, the solid curves are plotted over all $N \in [\![4, 256]\!]$. For the E-FO-Cantor, the dashed curve represented the theoretical relation $U_4 = N^{2\log_2 3}/6 - 1.5$.

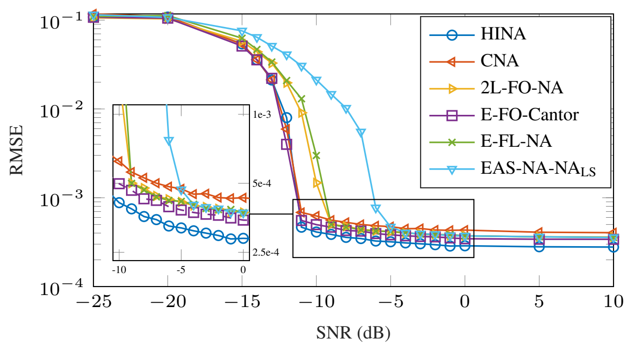

Fig. 3: The RMSE over SNR for the arrays in Table 1. There are $D = 13$ equal-powered sources with normalized DOAs $\bar{\theta}_d$ evenly distributed in $[-0.49, 0.49]$. The number of snapshots is 10^4. Each data point results from $R = 500$ Monte-Carlo trials.

and (22) we can assume without loss of generality $N_1^{\text{opt}} \geq N_2^{\text{opt}}$ and $N_3^{\text{opt}} \geq N_4^{\text{opt}}$. By the properties that no N_i and N_j can differ by more than 1 and that $N_2^{\text{opt}} \geq N_3^{\text{opt}}$, we write $N_i^{\text{opt}} = \bar{N} + \varepsilon_i$ for $i \in [\![1, 3]\!]$, and $N_4^{\text{opt}} = \bar{N}$, where $\bar{N}$ is some integer and $\varepsilon_1, \varepsilon_2, \varepsilon_3 \in \{0, 1\}$ with $\varepsilon_1 \geq \varepsilon_2 \geq \varepsilon_3$. By (19b), $4\bar{N} + (\varepsilon_1 + \varepsilon_2 + \varepsilon_3) = N = 4k + l$, where k and l are the quotient and the remainder of N divided by 4, respectively. Finally, by the uniqueness of the remainder and the fact that $\varepsilon_1 + \varepsilon_2 + \varepsilon_3 \in [\![0, 3]\!]$, $\varepsilon_1 + \varepsilon_2 + \varepsilon_3 = l$ and $\bar{N} = k$. The solution given in (20) is derived by discussing different values of l and taking into consideration the fact that $\varepsilon_1 \geq \varepsilon_2 \geq \varepsilon_3$. $\square$

As a remark, for sufficiently large N, the parameter U_4 of HINA has an asymptotic expression $U_{4,\text{HI}} \approx N^4/128$. This expression is a direct consequence of Theorem 2 and (19a).

4. NUMERICAL EXAMPLES

In this section, we compare several arrays, including HINA, CNA [11], 2L-FO-NA [12], E-FO-Cantor [13], E-FL-NA [10], and EAS-NA-NA$_{\text{LS}}$ [9], with respect to their U_4 and DOA estimation performance. Among these arrays, HINA, CNA, 2L-FO-NA, and E-FO-Cantor have hole-free $\mathbb{D}_4$. E-FL-NA and EAS-NA-NA$_{\text{LS}}$ have holes in their $\mathbb{D}_4$.

Table 1: Parameters for array configurations ($N = 8$)

Array	Parameters*	Sensors	U_4	Hole-free $\mathbb{D}_4$
HINA (Prop.)	(2,2,2,2)	{0,1,2,5,32,56,64,72}	144	Yes
CNA [11]	(4,6)	{0,1,3,4,9,27,45,54}	108	Yes
2L-FO-NA [12]	(4,4)	{0,1,2,3,35,42,49,56}	112	Yes
E-FO-Cantor [13]	2	{0,1,3,4,24,33,51,60}	120	Yes
E-FL-NA [10]	(3,3,2,3)	{1,2,3,6,9,26,68,110}	117	No
EAS-NA-NA$_{\text{LS}}$ [9]	(2,3,2,2)	{0,1,2,5,8,33,58,133}	141	No

*Parameters are either $(N_1, \ldots, N_m)$, $m \in [\![2, 4]\!]$ or r.

Fig. 2 compares the U_4 versus the number of sensors N. In Fig. 2 in the log-log scale, the slope of the curve of HINA is the same as those of the E-FL-NA and the EAS-NA-NA$_{\text{LS}}$ and is steeper than the others. This phenomenon validates that HINA, the E-FL-NA and the EAS-NA-NA$_{\text{LS}}$ possess $U_4 = \mathcal{O}(N^4)$. Among these arrays in Fig. 2, HINA is the only array with a hole-free $\mathbb{D}_4$ and $U_4 = \mathcal{O}(N^4)$ at the same time. In the zoom-in plot in Fig. 2, HINA owns the largest U_4 for $N \in [\![4, 9]\!]$ and the second largest U_4 for $N \in [\![10, 12]\!]$.

In Fig. 3, we compare the DOA estimation performance among the array configurations in Table 1. All these arrays have $N = 8$ sensors. There are $D = 13$ equal-powered sources, whose normalized DOAs $\bar{\theta}_d$ for $d \in [\![1, D]\!]$ are evenly distributed from -0.49 to 0.49. The source signals $s_d(t)$ for $d \in [\![1, D]\!]$ are 16-QAM symbol sequences modulated from D statistically independent random bit sequences. We apply the co-array MUSIC algorithm [22] on the Hermitian Toeplitz matrix associated with the fourth-order difference co-array. The number of snapshots is 10^4. The SNR is defined to be E_b/N_0, where $E_b := \mathbb{E}[|s_1(t)|^2]/\log_2 M$ with $M = 16$ being the number of different symbols, and $N_0 := \mathbb{E}[|n_1(t)|^2]$. The simulation is performed with $R = 500$ Monte-Carlo trials. The MSE at the rth trial is defined by $\text{MSE}^{(r)} := \frac{1}{D}\sum_{d=1}^{D}(\bar{\theta}_d - \hat{\bar{\theta}}_d^{(r)})^2$, where $\hat{\bar{\theta}}_d^{(r)}$ is the dth estimated DOA in the rth trial. Since there are outliers in $\text{MSE}^{(r)}$ caused by spurious peaks and missing peaks in the MUSIC spectrum, we first exclude the largest 3% and the smallest 3% $\text{MSE}^{(r)}$. Then we calculate the RMSE as the square root of the arithmetic mean of the remaining 94% $\text{MSE}^{(r)}$.

As SNR increases, the RMSE curves of all the arrays decrease. Moreover, HINA has the lowest RMSE among all the arrays for SNR no less than -11dB. Although the E-FO-Cantor also has a hole-free $\mathbb{D}_4$, the U_4 of HINA is 20% larger than that of the E-FO-Cantor, resulting in better DOA estimation performance. On the other hand, while the EAS-NA-NA$_{\text{LS}}$ has roughly the same U_4 as HINA, HINA outperforms the EAS-NA-NA$_{\text{LS}}$ due to the hole-free $\mathbb{D}_4$ of HINA.

5. CONCLUDING REMARKS

This paper proposed the half inverted nested array (HINA). Based on the closed-form expression for the optimal parameters, HINA enjoys a hole-free fourth-order difference co-array of size $\mathcal{O}(N^4)$. Numerical examples demonstrated the U_4 of HINA and the improved DOA estimation performance of HINA.

A future direction is to construct new sparse arrays whose hole-free $\mathbb{D}_4$ is larger than that of HINA [23]. Furthermore, a $2q$th-order generalization of HINA with a hole-free $2q$th-order difference co-array of size $\mathcal{O}(N^{2q})$ is also of interest for $q > 2$.

6. REFERENCES

[1] M. Ibrahim, F. Römer, R. Alieiev, G. Del Galdo, and R. S. Thomä, "On the estimation of grid offsets in CS-based direction-of-arrival estimation," in *2014 IEEE International Conference on Acoustics, Speech and Signal Processing (ICASSP)*, 2014, pp. 6776–6780.

[2] L. Pallotta, G. Giunta, and A. Farina, "DOA refinement through complex parabolic interpolation of a sparse recovered signal," *IEEE Signal Processing Letters*, vol. 28, pp. 274–278, 2021.

[3] T. E. Tuncer and B. Friedlander, *Classical and Modern Direction-of-Arrival Estimation*, Academic Press, Inc., USA, 2009.

[4] H. L. Van Trees, *Optimum Array Processing: Prat IV of Detection, Estimation, and Modulation Theory.*, Hoboken, NJ, USA: Wiley, 2002.

[5] H. Krim and M. Viberg, "Two decades of array signal processing research: the parametric approach," *IEEE Signal Processing Magazine*, vol. 13, no. 4, pp. 67–94, 1996.

[6] P. Pal and P. P. Vaidyanathan, "Multiple level nested array: An efficient geometry for $2q$th order cumulant based array processing," *IEEE Transactions on Signal Processing*, vol. 60, no. 3, pp. 1253–1269, 2012.

[7] S. Shamsunder and G. B. Giannakis, "Modeling of non-gaussian array data using cumulants: Doa estimation of more sources with less sensors," *Signal Processing*, vol. 30, no. 3, pp. 279–297, 1993.

[8] M.C. Dogan and J.M. Mendel, "Applications of cumulants to array processing .i. aperture extension and array calibration," *IEEE Transactions on Signal Processing*, vol. 43, no. 5, pp. 1200–1216, 1995.

[9] Y. Zhou, J. Li, W. Nie, and Y. Li, "The fourth-order difference co-array construction by expanding and shift nested array: Revisited and improved," *Signal Processing*, vol. 188, pp. 108198, 2021.

[10] Q. Shen, W. Liu, W. Cui, S. Wu, and P. Pal, "Simplified and enhanced multiple level nested arrays exploiting high-order difference co-arrays," *IEEE Transactions on Signal Processing*, vol. 67, no. 13, pp. 3502–3515, 2019.

[11] Y. Zhou, Y. Li, L. Wang, C. Wen, and W. Nie, "The compressed nested array for underdetermined DOA estimation by fourth-order difference coarrays," in *ICASSP 2020 - 2020 IEEE International Conference on Acoustics, Speech and Signal Processing (ICASSP)*, 2020, pp. 4617–4621.

[12] A. Ahmed, Y. D. Zhang, and B. Himed, "Effective nested array design for fourth-order cumulant-based DOA estimation," in *2017 IEEE Radar Conference (RadarConf)*, 2017, pp. 0998–1002.

[13] Z. Yang, Q. Shen, W. Liu, Y. C. Eldar, and W. Cui, "Extended Cantor arrays with hole-free fourth-order difference co-arrays," in *2021 IEEE International Symposium on Circuits and Systems (ISCAS)*, 2021, pp. 1–5.

[14] D. Manolakis, V. Ingle, and S. Kogon, *Statistical and Adaptive Signal Processing: Spectral Estimation, Signal Modeling, Adaptive Filtering and Array Processing*, New York, NY, USA: McGraw-Hill, 2000.

[15] Q. Shen, W. Liu, W. Cui, and S. Wu, "Extension of nested arrays with the fourth-order difference co-array enhancement," in *2016 IEEE International Conference on Acoustics, Speech and Signal Processing (ICASSP)*, 2016, pp. 2991–2995.

[16] J. Cai, W. Liu, R. Zong, and Q. Shen, "An expanding and shift scheme for constructing fourth-order difference coarrays," *IEEE Signal Processing Letters*, vol. 24, no. 4, pp. 480–484, 2017.

[17] P. Pal and P. P. Vaidyanathan, "Nested arrays: A novel approach to array processing with enhanced degrees of freedom," *IEEE Transactions on Signal Processing*, vol. 58, no. 8, pp. 4167–4181, 2010.

[18] C.-L. Liu and P. P. Vaidyanathan, "Remarks on the spatial smoothing step in coarray music," *IEEE Signal Processing Letters*, vol. 22, no. 9, pp. 1438–1442, 2015.

[19] V. P. Leonov and A. N. Shiryaev, "On a method of calculation of semi-invariants," *Theory of Probability & Its Applications*, vol. 4, no. 3, pp. 319–329, 1959.

[20] R. Rajamäki and V. Koivunen, "Sparse symmetric linear arrays with low redundancy and a contiguous sum co-array," *IEEE Transactions on Signal Processing*, vol. 69, pp. 1697–1712, 2021.

[21] S. Ren, T. Zhu, and J. Liu, "Generalized design approach for fourth-order difference co-array," in *2018 International Conference on Radar (RADAR)*, 2018, pp. 1–5.

[22] S.U. Pillai, Y. Bar-Ness, and F. Haber, "A new approach to array geometry for improved spatial spectrum estimation," *Proceedings of the IEEE*, vol. 73, no. 10, pp. 1522–1524, 1985.

[23] Y.-P. Chen and C.-L. Liu, "Half inverted design scheme for large hole-free fourth order difference co-arrays," *In preparation.*